Pulse-to-pulse stability analysis in a frequency-doubled, q-switched Nd:YAG rod-Laser

Matheus A. Tunes[a1], Cláudio G. Schön[a], Niklaus Ursus Wetter[b]

[a]Escola Politécnica da Universidade de São Paulo, Av. Prof. Mello de Moraes 2463, Cid. Universitária, São Paulo, SP - Brazil 05508-030

[b]Instituto de Pesquisas Energéticas e Nucleares - CNEN, Av. Prof. Lineu Prestes 2242, Cid. Universitária, São Paulo, SP - Brazil 05508-000

ABSTRACT

Bistability was observed in a frequency-doubled and q-switched Nd:YAG rod-Laser. When the same cavity contains a quarter-wave plate (QWP) no such bistability is observed and higher output powers are obtained. By means of a Monte-Carlo simulation of the rate equations we achieve good agreement with the observed behavior.

Keywords: Pulse-to-pulse power stability; Quarter-wave plate; Monte-Carlo Simulation; Nd:YAG rod-Laser.

1. INTRODUCTION

The q-switched Nd:YAG Laser is widely used in medical, industrial and scientific applications because it is an excellent and efficient source for short duration, high-energy and high beam-quality Laser pulses [1-5]. For many applications, especially of the industrial and scientific kind, it is of great importance that the temporal pulse shape as well as its amplitude remains constant throughout the experiment. Additionally the Laser system should be compact and cheap and, therefore, very efficient, which requires a high gain system. For example in traditional Nd:YAG resonators that use gain crystals in the form of rods that are pumped laterally by lamps or semiconductor diodes, the highest output power is generally obtained by using multiple transverse resonator modes which exploit the whole gain volume and therefore occupy the whole rod [6]. Such high mode-volume Lasers can be easily achieved by using a plane-plane resonator and although this resonator operates at the edge of the stability interval, the thermally induced lens of positive focal length tends to stabilize the resonator.

However, the thermal effects have also negative properties such as thermally induced stress birefringence, which is especially strong in high mode-volume Lasers [7]. The latter effect results in changes of the beam's polarization state which hampers the Lasers efficiency and pulse-to-pulse stability for second harmonic generation (SHG). Such frequency doubled Nd:YAG Lasers operate normally at 532 nm and have become the workhorse for many medical, industrial and scientific applications. They generally rely on a linear polarization state in order to generate high efficiencies upon frequency conversion in SHG crystals [8]. The polarization direction is normally fixed by an intra-cavity polarization plate such as a quartz window at Brewster angle.

In Nd:YAG rods the thermally induced birefringence is radial and tangential with respect to the optical axis at the center of the rod. For a linear polarized beam entering the rod under thermal stress this will cause those parts of the beam that are not purely radially (along the polarization axis) or tangentially (perpendicular to the polarization axis) polarized to

[1] matheus.tunes@ctmsp.mar.mil.br || http://lasergroup.wix.com/ldl || office phone +55 11 3817 7612 ||

Instrumentation, Metrology, and Standards for Nanomanufacturing, Optics, and Semiconductors VII, edited by Michael T. Postek, Ndubuisi George Orji, Proc. of SPIE Vol. 8819, 88190G
 · doi: 10.1117/12.2025847

acquire an elliptical polarization state. These elliptically polarized regions of the beam will consequently suffer strong losses at the intra-cavity polarization plate [7].

It has been shown that the usage of a quarter-wave-plate in a standing-wave resonator can almost completely restore the beam's original polarization state when its axis is aligned with the intra-cavity polarizer thereby decreasing the losses suffered because of thermal birefringence [9-10]

The thermo-optic instabilities also cause additional pulse-to-pulse energy oscillations in the case of resonators that are q-switched because of the absence of a steady-state and because of the necessary high inversion populations that favor non-linear population mechanisms. It is therefore of fundamental importance to carry out a meticulous pulse-to-pulse energy and time stability characterizations, for example using pulse-to-pulse statistics. To the best of our knowledge in the scientific literature there is no standard method to estimate the pulse-to-pulse stability. Most researchers chooses to operate the Laser for hours and analyze the pulse energy behavior (or frequency [11]) in a form of a temporal series. Others [12-13] just observe the pulse average power stability measuring the amplitude fluctuations in a successive pulse collection, since the amplitude is related to pulse energy. Although these techniques give us some information regarding pulse stability, they do not provide quantitative measures of pulse-to-pulse energy fluctuations.

In this paper we analyze the pulse-to-pulse fluctuations in a collection of pulse area histograms. The statistical approach allows us to estimate the stability in terms of the histogram's standard deviation (SD). The lower the SD the higher is the energy stability. This methodology has been applied to perform a stability characterization of a plane-plane Nd:YAG Laser resonator, passively q-switched and frequency-doubled to 532 nm. We analyze two different Laser set-ups: with and without quarter-wave plate inside the resonator. In the first case Gaussian histograms were obtained whereas in the latter case bistability was observed in the pulse energy histograms. We apply a Monte-Carlo simulation, using the rate equation for the q-switched regime, to reproduce some aspects of the experimentally measured pulse bistability.

2. THEORETICAL APPROACH

2.1 Q-switching Rate equations

The parameters used to characterize the laser are the density of active ions in the laser rod N_0, the spontaneous decay lifetime τ_l, the absorption coefficient α_0, the volume V and the length l of the rod, the physical size of the cavity L, the photon density ϕ at the frequency υ and the fractional photon losses γ (DC and AC losses due to output coupling and saturable absorber) [14].

In the model, the photon amplification coefficient is represented by

$$\alpha = \frac{\alpha_0 N}{N_0} \tag{1}$$

for a population inversion of N, giving a single pass photon generation rate of $\phi\alpha l$. Considering the fact that the photons are lost at a rate of ϕ/τ where τ is the photon lifetime, we write the first rate equation for the photon density:

$$\frac{d\phi}{dt} = \left(\frac{\alpha l}{t_1} - \frac{1}{\tau}\right)\phi \tag{2}$$

where $t_1 = L/c$ is the single pass transit time. If we also neglect the pumping term, we can write a second equation for the rate of the population inversion:

$$\frac{dN}{dt} = -\frac{2\alpha l}{t_1}\phi \tag{3}$$

Renormalizing our system of equations by introducing $n = N/N_0$, the fractional population inversion, and $\varphi = \phi/N_0$, we obtain

$$\begin{cases} \dfrac{d\phi}{dt} = \left(\dfrac{\alpha_0 N l}{N_0 t_1} - \dfrac{1}{\tau}\right)\phi \\ \dfrac{1}{N_0}\dfrac{dN}{dt} = -\dfrac{2\alpha_0 N l}{N_0 t_1}\phi/N_0 \end{cases} \xrightarrow{yields} \begin{array}{l} \dfrac{d\varphi}{dt} = \left(\dfrac{\alpha_0 l}{t_1} n - \dfrac{1}{\tau}\right)\varphi \\ \dfrac{dn}{dt} = -\dfrac{2\alpha_0 l}{t_1} n\varphi \end{array} \tag{4}$$

Finally, we perform a change in the timescale $dt = \tau dt'$ to obtain τ as unit of time, observing the loss coefficient in the system:

$$\begin{cases} \dfrac{d\varphi}{dt} = \left(\dfrac{\alpha_0 l}{\gamma} n - 1\right)\varphi \\ \dfrac{dn}{dt} = -\dfrac{2\alpha_0 l}{\gamma} n\varphi \end{cases} \tag{5}$$

The term $\gamma/\alpha_0 l$ is rewritten as a new parameter n_p:

$$\begin{cases} \dfrac{d\varphi}{dt} = \left(\dfrac{n}{n_p} - 1\right)\varphi \\ \dfrac{dn}{dt} = -\dfrac{2n}{n_p}\varphi \end{cases}, \qquad n_p = \frac{\gamma}{\alpha_0 l} \tag{6}$$

In the scientific literature the n_p parameter is known as population inversion threshold. The dynamic system (6) of these two differential equations regulates the whole q-switching mechanism to achieve a giant pulse of high energy and short duration as well reported in the literature [14].

The n_p parameter deserves a special attention: Despite the fact that there is a deterministic solution for this system, the fluctuations of the photon losses add a stochastic nature to the q-switching process, specifically to the pulse-to-pulse generation. Each pulse may have a slightly different behavior that can be represented by randomness in the n_p parameter limiting the analytical solution of the system as well as its accuracy regarding pulse-to-pulse power stability. In this way, we can rewrite the Q-switching rate equations to perform a Monte-Carlo simulation aimed at reproducing the bistable pulse behavior.

Many reasons may contribute to instability of pulse energy inside a Nd:YAG rod-Laser. As stated above, thermo-mechanical and thermo-optical effects are the main causes of such instabilities. Additionally, the plane-parallel resonator adds to the instability because of its unstable nature. To compare quantitatively the difference in terms of stability of both resonators, with and without quarter-wave plate, we introduce the following ratio which uses the standard deviations of the pulse area histograms:

$$\eta = \left(1 - \frac{\sigma_{withL4}}{\sigma_{withoutL4}}\right) \cdot 100[\%] \tag{7}$$

3. EXPERIMENTAL SET-UP

In our work we used a plane-parallel resonator containing a Nd:YAG rod of 7 cm length and 3 mm diameter, side-pumped by 12 diode bars. The pulse rate was 10 Hz with 120 microseconds pulse width. The total diode pump power was 1200 Watts and a water chiller was used to cool the rod. For Q-switching generation, we inserted an intra-cavity

saturable absorber crystal (Cr^{+4}:YAG) of 50% initial absorption and, after the 20% output coupler, a KTP crystal was placed for second harmonic generation thus achieving the 532 nm wavelength of our Laser. The quarter-wave plate was placed before the totally reflective back-mirror and the Brewster window before the output coupler. A fast detector and a high-bandwidth oscilloscope (LeCroy, model WaveRunner 104MXi) were used for data processing, statistical analysis (histograms) and storage. A diffusor was placed 10 cm before the detector in order to avoid any influence of the lasers modal intensity distribution on the measurement.

The pulse characterization was performed for different pump-rate frequencies ranging from 10 to 100 Hz. Pulse area histograms integrating over 10.000 pulses were collected, although the SD of the histogram would remain approximately the same after only a few pulses (around 10 pulses) until the end of the acquisition time.

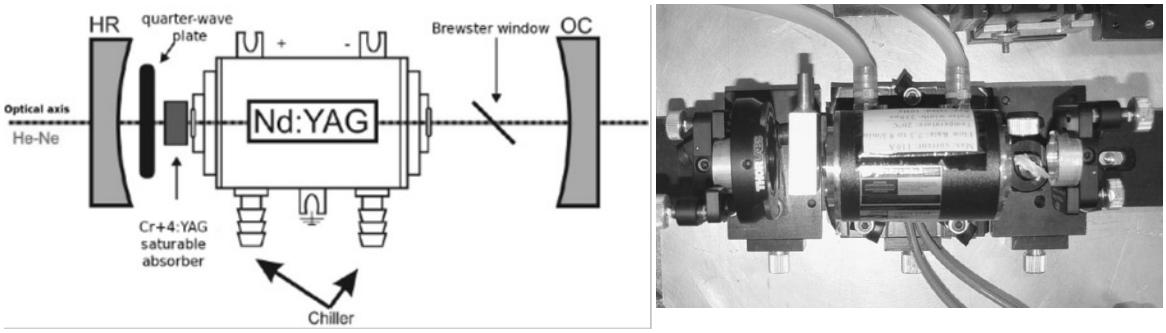

Figure 1: The experimental Laser set-up employed in our experiments.

4. RESULTS

Bistability was observed for pump rates of 10 Hz and 60 Hz, always without quarter-wave plate inside the cavity. Figure 2 shows the 60 Hz pump-rate case without (left) and with (right) quarter-wave plate inside cavity. At other pulse repetition frequencies we observe a strong asymmetrical pulse area histogram for the resonator without quarter-wave plate. An example of the strong asymmetric case without bistability is shown in the next figure corresponding to 50 Hz pulse repetition rate:

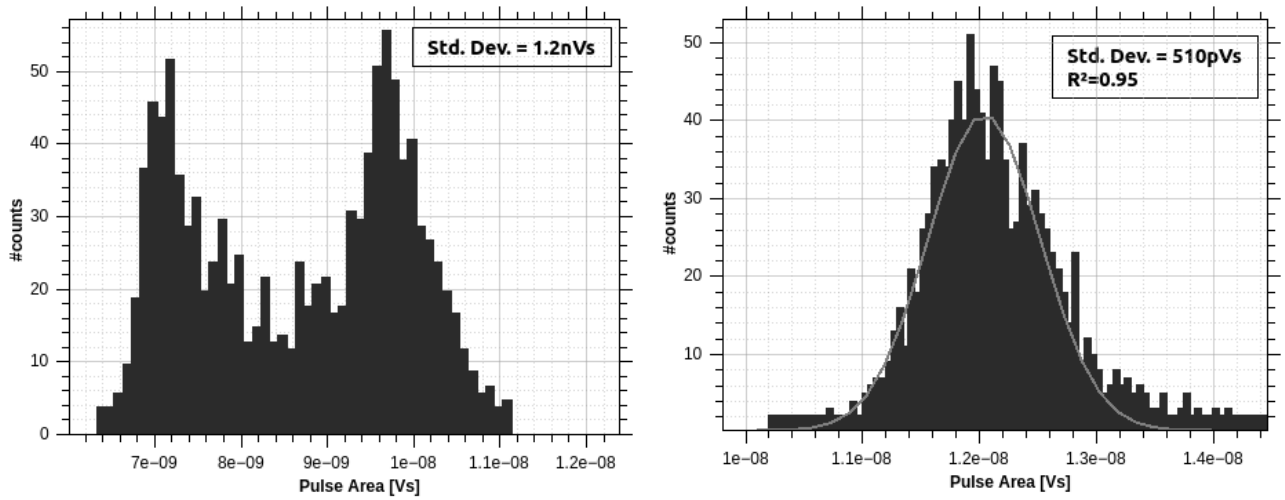

Figure 2: Pulse area histogram corresponding to a 60 Hz pump-rate. Left image without quarter-wave plate inside cavity and right image with quarter-wave plate inside.

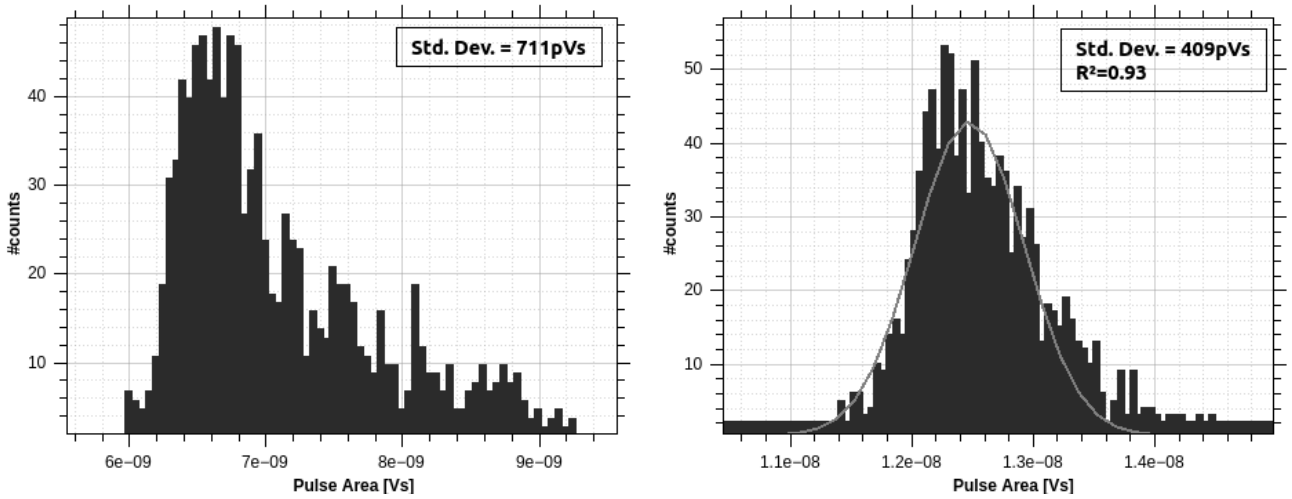

Figure 3: Pulse area histogram corresponding to 50 Hz of pump-rate. As in this case all histograms without quarter-wave plate exhibit a strong asymmetric shape. Left is the case without quarter-wave plate and right with the plate inside cavity.

Table 1 summarizes our main results regarding pulse area distribution. The classification type is the symmetry type of distributions: asymmetric, strong asymmetric with tail (like the left of figure 3), bistable (like the left of figure 2) and symmetric (typical Gaussian curve like all cases with quarter-wave plate).

Table I: Pulse area histograms distributions.

Pump-rate Frequency [Hz]	Std. Dev. Without QWP	Histogram type	Std. Dev. With QWP	Histogram type	Efficiency
10	397 pVs	Strong symmetric	553 pVs	Symmetric	**N/A**
20	692 pVs	Bistable	485 pVs	Symmetric	**29,91%**
30	570 pVs	Asymmetric	510 pVs	Symmetric	**10,53%**
40	465 pVs	Asymmetric	500 pVs	Symmetric	**N/A**
50	711 pVs	Strong asymmetric	489 pVs	Symmetric	**31,22%**
60	1.2 nVs	Bistable	510 pVs	Symmetric	**57,20%**
70	394 pVs	Asymmetric	549 pVs	Symmetric	**N/A**
80	444 pVs	Strong asymmetric	659 pVs	Symmetric	**N/A**
90	658 pVs	Strong asymmetric	599 pVs	Symmetric	**8,97%**
100	405 pVs	Strong asymmetric	602 pVs	Symmetric	**N/A**
Data Dispersion	**247 pVs**	All asymmetric	**58 pVs**	All symmetric	**77% most efficient with L4**

When the quarter-wave plate is inserted into the cavity, we not only observe a smaller standard deviation, but also a strong increase in output power, which can be inferred from the scale of the x-axis of the pulse area histograms in the figures above. The figure 4 shows this situation from 10 to 500 Hz of pump-rate.

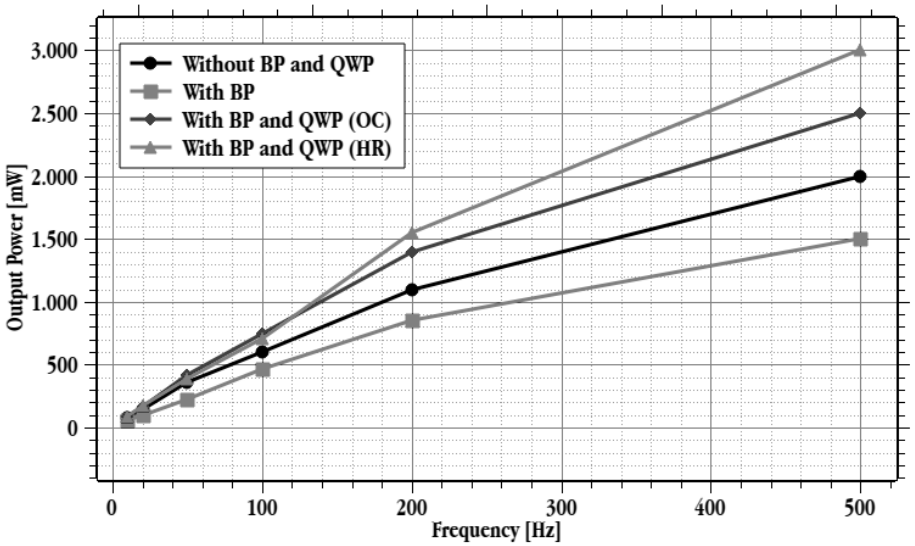

Figure 4: (Left) The output power as a function of pump-rate frequency. The data with BP (Brewster Plate) and QWP were taken with the QWP placed near to the Output Coupler (OC) or the High Reflector Mirror (HR).

Our simulation was carried out in a MATLAB environment to generate random variables that are then multiplied with the n_p loss parameter in order to represent the pulse-to-pulse variation of the losses. In a next step, photon density and population inversion are calculated (equation (6)) using a standard Runge-Kutta integration. The simulation produces two curves that represent the photon density ϕ (solid line) and the population inversion (dotted line) as presented in figure 5. The x-axis is in units of τ and does not present the "detector time" of our experiments. These results are then grouped in the histograms of figure 6, which are over 500 pulses. Clearly seen is the appearance of a bistability for high values of the MC parameter, corresponding to high fractional losses.

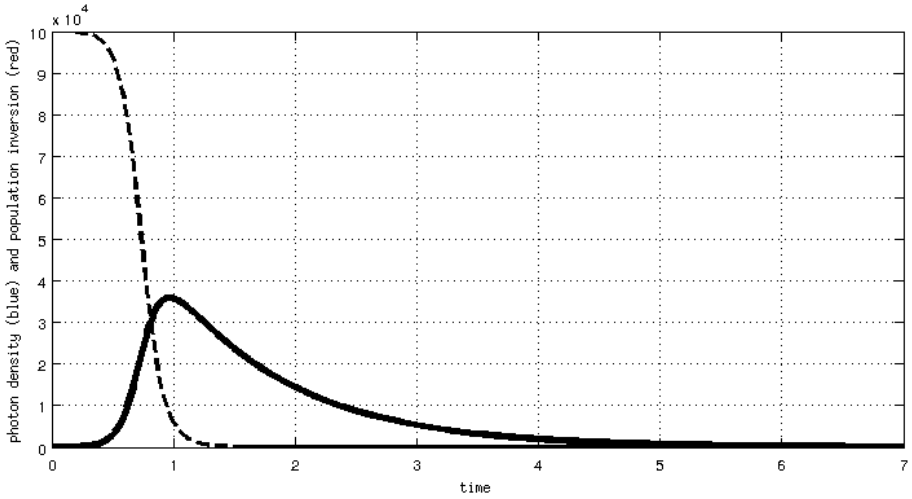

Figure 5: Simulation of the Q-switched system: photon density $\boldsymbol{\varphi}$ (straight line) and inversion density $\boldsymbol{n}$ (dotted line).

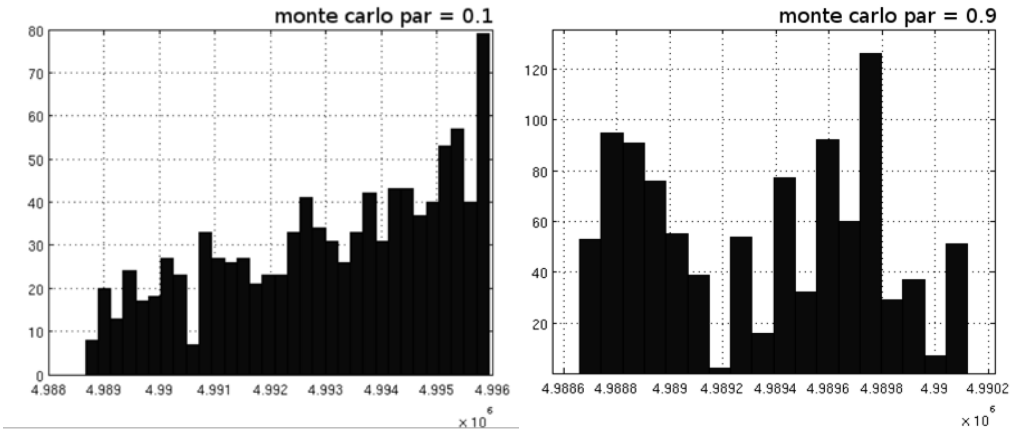

Figure 6: Histograms obtained by Monte Carlo simulation (MC) integrating over 500 pulses. The MC parameter refers to the loss percentage in the system. Bistability is observed when the MC parameter reaches a value of 0.9.

5. CONCLUSION

The characterization of a pulsed Laser based on statistical analysis of the pulse area histograms is a very fast characterization of the Lasers stability since it permits to visualize if there is bistability or asymmetry in the histogram (and therefore a large standard deviation) after only a few seconds (when operating at rep rates above 10 Hz). This is in contrast to other techniques aforementioned that register the Lasers output power (amplitude fluctuations/trends) and need much more time. It is therefore a good tool to compare the stability of different resonator configurations and under different alignment conditions.

As indicated in figure 2 we obtained an enhancement of 57% in the Laser's pulse energy when operated with the quarter-wave plate at 60 Hz compared to without QWP. Additionally, the standard deviation is reduced by one order of magnitude, indicating that resonator operates with much more stability.

In all cases we have lower data dispersion when the quarter wave-plate is present. Observing the standard deviations from table I, we note that the data dispersion of all the standard deviations of histograms with QWP is 58 pVs when the quarter-wave plate is present and 247 pVs without QWP.

The histograms in the figure 6 show us that bistability may be reproduced by the MC simulation in cases where the losses reach a high value as represented by the MC parameter of 0.9 in our simulation.

REFERENCES

[1] Simeonsson, J.B., Williamson, L.J. "Characterization of Laser induced breakdown plasmas used for measurements of arsenic, antimony and selenium hydrides," Spectrochimica Acta Part B: Atomic Spectroscopy 66, 754-760 (2011).

[2] Luo, W.F. et al. "Characteristics of the aluminum alloy plasma produced by a 1064 nm Nd : YAG Laser with different irradiances," Pramana 74, 945-959 (2010).

[3] McManamon, P.F., Kamerman, G. & Huffaker, M. "A history of Laser radar in the United States," Laser Radar Technology and Applications XV 7684, 76840T-76840T-11 (2010).

[4] Petrova-Mayor, A., Wulfmeyer, V. & Weibring, P. "Development of an eye-safe solid-state tunable Laser transmitter in the 1.4-1.5 μm wavelength region based on Cr4+:YAG crystal for lidar applications," Applied Optics 47, 1522 (2008).

[5] Nagasawa, A. "New diagnostic method for dental caries applying photothermal reaction on teeth to Nd:YAG Laser irradiation," Proceedings of SPIE 2163, 413-421 (1994).

[6] Magni, V; et at. "Q-switched Nd:YAG Laser with super-gaussian resonator," Optics Letters 16, 642-644 (1991).

[7] Koechner, W. "Thermal Lensing in a Nd:YAG Laser Rod," Applied Optics 9, 2548 (1970).

[8] Kaminski, A., [Laser Crystals], Nauka, Moscow, (1975).

[9] Scott, W.C. "Birefringence Compensation and TEM00 mode enhancement in a Nd:YAG Laser," Applied Physics Letters 18, 3 (1971).

[10] Clarkson, W.A., Felgate, N.S. & Hanna, D.C. "Simple method for reducing the depolarization loss resulting from thermally induced birefringence in solid-state Lasers," Optics Letters 24, 820 (1999).

[11] Wu, F.-T. & Zhang, W.-Z. "High energy and high stability Cr4+:YAG passively Q-switched Laser with convex-ARR unstable resonator," Optics & Laser Technology 32, 107-110 (2000).

[12] Zhou, B., Kane, T.J., Dixon, G.J. & Byer, R.L. "Efficient, frequency-stable Laser-diode-pumped Nd:YAG Laser," Optics Letters 10, 62 (1985).

[13] Chen, F. et al. "Diode-pumped acousto-optically Q-switched high-repetition-rate Nd:YAG Lasers at 946 and 473 nm by intracavity frequency-doubling," Laser Physics 22, 81-86 (2011).

[14] Wagner, W. and Lengyel, A. "Evolution of the Giant Pulse in a Laser," Journal of Applied Physics v.34(7), pp. 2040-2046 (1963).